JACS
JOURNAL OF THE AMERICAN CHEMICAL SOCIETY

COMMUNICATION

pubs.acs.org/JACS

Biomimetic Crystallization of Ag_2S Nanoclusters in Nanopore Assemblies

Roberto de la Rica* and Aldrik H. Velders*

Laboratory of Supramolecular Chemistry and Technology, Faculty of Science and Technology, MESA+ Research Institute for Nanotechnology, MIRA Institute for Biomedical Technology and Technological Medicine, University of Twente, P.O. Box 217, 7500 AE Enschede, The Netherlands

Supporting Information

ABSTRACT: Self-organized nanocrystal architectures with subnanometric spatial resolution were obtained by mimicking the biological crystal growth. The key step of this facile, one-pot, biomimetic route is to induce the self-assembly of the artificial nanopore cucurbit[7]uril with metal ions, which generates supramolecular aggregates that recreate the physicochemical environment of biomineralization processes. The approach holds great promise for the fabrication of nanocrystal superstructures of functional materials, useful in optics, electronics, and catalysis.

The capability to organize matter at the nanoscale is raising great expectations for the fabrication of complex devices with outstanding functions.[1,2] While top-down nanofabrication requires sophisticated technologies, in biological systems the self-organization of nanometric building blocks is an ubiquitous phenomenon,[3] which has created a large interest in adapting these biological processes for the fabrication of inorganic structures with nanometric resolution.[4] For example, biomineralizing organisms such as marine sponges and sea urchins have evolved the capability to grow superstructures of perfectly aligned nanocrystals,[5] and replicating this phenomenon ex vivo could yield nanocrystal architectures that are spatially organized with exquisite accuracy.[6] In biomineralization, a widespread strategy to generate nanocrystal superstructures is to confine the nucleation of the nascent nanoparticles in a biological matrix that guides the alignment of the nanocrystal building blocks.[7] In the past, these biological conditions were successfully mimicked via the utilization of biological and artificial polymers that possess great affinity for metal ions and generate scaffolds where the infiltration of the precursors of the reaction is diffusion-limited.[8] Also, biological nanopores such as peptide nanorings[22] and toroidal DNA[23] could guide the growth and alignment of nanocrystals in vitro. In this communication, we report the mimicking of these conditions by using an artificial nanopore (cucurbit[7]uril, CB[7], Scheme 1) as the building block of biomimetic matrix for crystal growth. As a proof of concept of this biomimetic route, we grew nanoclusters of perfectly aligned Ag_2S nanocrystals in aqueous solution. Ag_2S is a perfect test material because polydisperse particles of varying shapes and poor crystallinity are usually obtained in aqueous solution due to the ultralow solubility of this material in water.[11] Moreover, it is a very interesting material with applications in optics[12] and nanomedicine.[13] Here, we report on the facile fabrication in water of self-organized Ag_2S nanocrystal superstructures with subnanometric spatial resolution by simply triggering the self-assembly of the nanopore with Ag^+ (step 1 in Figure 1), and adding S^{2-} to the resulting nanopore assemblies (step 2 in Figure 1).

Scheme 1. Schematic Representation of the Artificial Nanopore Cucurbit[7]uril (CB[7]), Showing the Repeating Unit[a]

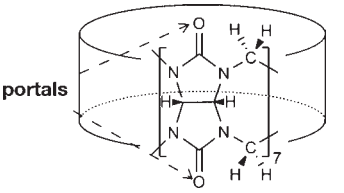

[a] The carbonyl groups at the portals can establish ion−dipole interactions with cations. The cavity has a diameter of 7.3 Å[9] and can host a wide variety of guest molecules.[10]

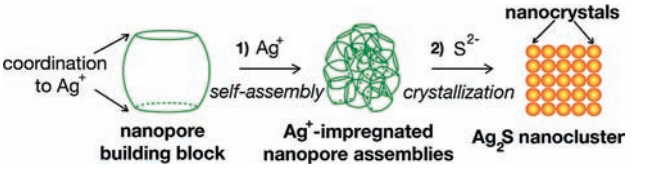

Figure 1. Scheme of the biomimetic fabrication of Ag_2S nanoclusters. (1) The assembly of the nanopore is triggered by adding Ag^+; (2) the nanopore assemblies guide the growth of nanocrystal superstructures (Ag_2S nanoclusters).

To demonstrate the formation of nanopore assemblies as biomimetic matrices for crystal growth (step 1 in Figure 1), we first studied the light-scattering behavior of the nanopore solution in the presence of Ag^+. In Figure 2a, the extinction of the nanopore sample measured at 600 nm, where none of the single components show any particular absorbance, increases as the concentration of Ag^+ increases. This observation is attributed to the larger size of nanopore assemblies compared to the initial building blocks.[14] In Figure 2b, atomic force microscopy (AFM) imaging and height profiles of the nanopore assemblies revealed nanostructures with a size distribution plot centered at 20 nm (inset in Figure 2b, additional image as Figure S1 online). In Figure 2c, Fourier transform infrared (FT-IR) spectroscopy experiments show that the peak corresponding to the carbonyl

Received: November 16, 2010
Published: February 14, 2011

   dx.doi.org/10.1021/ja110272g | J. Am. Chem. Soc. 2011, 133, 2875–2877

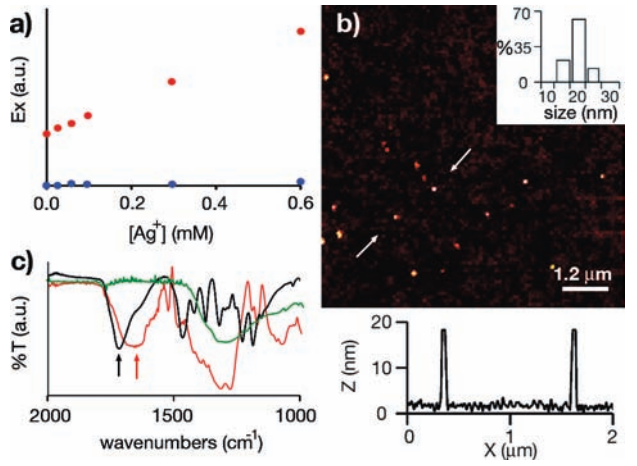

Figure 2. Self-assembly of the nanopore triggered by Ag^+. (a) Extinction (Ex) versus Ag^+ concentration in the presence (red) or in the absence (blue) of the nanopore (1 mM); (b) AFM image (topography) and height profile (indicated by arrows) of nanopore assemblies; (up-right inset) size distribution plot measured from height profiles; (c) FT-IR spectra of the nanopore (CB[7], black), nanopore assemblies (CB[7] + $AgNO_3$, red) and the silver salt ($AgNO_3$, green). The peak corresponding to the carbonyl groups of CB[7] is indicated by arrows.

groups of the nanopore broadens and shifts from 1716 cm^{-1} to 1655 cm^{-1}, which indicates that these carbonyl groups coordinate metal ions in the nanopore assemblies.[15] This observation is in agreement with previously published data on the interaction of the carbonyl groups of CB[7] with Ag^+.[16] The above-mentioned results demonstrate that the nanopore assembles in the presence of Ag^+ via coordination of the metal ion to carbonyl groups at the portals, which results in the formation of Ag^+-impregnated nanopore assemblies.

After proving the formation of the biomimetic matrix, the growth of Ag_2S crystals was studied by adding thioacetamide as source of S^{2-} to the solution containing the nanopore assemblies (step 2 in Figure 1). After 24 h incubation time, nanoclusters with a granular appearance were observed by high-resolution transmission electron microscopy (HRTEM, Figure 3a and Figure S3 online), whose constituent nanocrystals had a diameter of <1 nm. The size distribution plot of the nanoclusters centered at 20 nm (up-right inset in Figure 3a) matches well the size of the nanopore assemblies in Figure 2c, in accordance with the idea that the nanoclusters are grown in the nanopore assemblies. The selected-area electron diffraction (SAED) pattern of a group of nanoclusters (down-left inset in Figure 3a) shows the (120), (112), and (−212) faces of monoclinic α-Ag_2S (JCPDS card 14-0072), which is the most stable polymorph at room temperature. To confirm our HRTEM observations that the nanoclusters in Figure 3a are made of smaller nanocrystals, the optical properties of the nanocluster solution were queried with UV−vis spectroscopy. It is well established that below a critical size value semiconducting materials enter the quantum confinement regime, and their absorbance shows a blue shift as the size of the nanocrystals decreases.[17] In Figure 3b, the absorption spectrum reveals a peak centered at 500 nm, which was not found when the reaction was performed in the absence of the nanopore or in the precursors of the reaction (Figure S2 online). This value is blue-shifted with respect to the absorption peak reported for Ag_2S nanocrystals with a diameter of 10.2 nm,[18] which confirms that the nanoclusters are made of individual nanocrystals of smaller size.

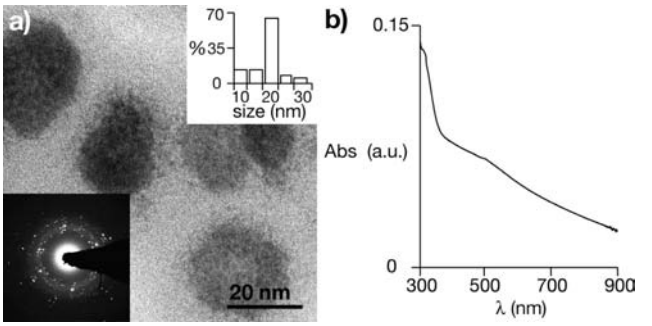

Figure 3. Nanoclusters of Ag_2S nanocrystals. (a) HRTEM image showing nanoclusters of Ag_2S nanocrystals; (up-right inset) size distribution plot (diameter); (down-left inset) SAED pattern; (b) UV−vis spectrum of the nanocluster solution.

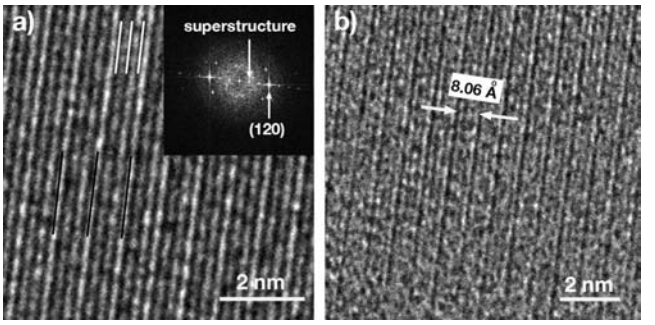

Figure 4. Nanocrystal superstructure. (a) High-magnification HRTEM image showing the lattice fringe of the (120) face (highlighted with white lines) and the superstructure (highlighted with black lines); (up-right inset) Fourier diffractogram; (b) HRTEM image showing the superstructure after applying a small defocus.

While in Figure 3 we demonstrated the growth of Ag_2S nanoclusters in the solution containing nanopore assemblies, information about the spatial arrangement of the constituent nanocrystals cannot be extracted from low-magnification images. Figure 4a shows a high-magnification HRTEM image obtained from a nanocluster, where the lattice fringe of the face (120) crosses the whole structure with no apparent misalignment (Figure S4 online). In this image, another periodic structure with a pitch of 8.06 Å was found parallel to the lattice fringe of the face (120) (highlighted with black lines in Figure 4a, see also Figure S5 online). This periodicity, which became more evident upon application of Fourier transformation (inset in Figure 4a) or a small defocus (Figure 4b and Figure S6 online), cannot be ascribed to the crystalline structure of monoclinic α-Ag_2S, and hence it must be the consequence of a nanocrystal-based superstructure.[19] These results demonstrate that the constituent Ag_2S nanocrystals are aligned in the nanocluster to yield self-organized architectures with subnanometric spatial resolution.

Above, we demonstrated that nanoclusters of perfectly aligned Ag_2S nanocrystals were grown by simply adding a self-assembling nanopore to the metal ion solution and triggering the crystallization with the anion precursor (Figure 1). This outstanding control over the crystallization of a material as insoluble in water as Ag_2S was made possible by mimicking the crystallization of biominerals in organic matrices, which generates nanocrystal superstructures. Although the exact mechanism underlying this nanoparticle-based crystallization pathway is not fully understood yet,[6] several conditions have been extensively proved by

dx.doi.org/10.1021/ja110272g | J. Am. Chem. Soc. 2011, 133, 2875–2877

other groups to be essential in this process. For example, in many cases, the presence of functional groups with great affinity for metal ions promotes local supersaturation in a polymer matrix, and this condition is crucial for obtaining nanoparticle-based superstructures.[20] In the present work this condition is fulfilled via coordination of Ag^+ to the carbonyl groups of the nanopore (Figure 2b), which generates assemblies with internalized metal ions. Moreover, the presence of nanopores in the assemblies is important to control mass transport of precursors, which is also a well-established requirement for biomimetic crystallization.[8,21] To demonstrate this point, we occluded the nanopores in the assemblies with a small organic molecule, benzene, and repeated the same synthetic procedure. When the optical properties of the solution were queried with UV−vis spectroscopy, the characteristic peak of small Ag_2S nanocrystals with a diameter of <1 nm was not found (Figure S7 online), which demonstrated that infiltration of the precursors of the reaction through the nanopores is a key factor to obtain nanocrystal superstructures.

In conclusion, we demonstrated the synthesis of nanoclusters of perfectly aligned Ag_2S nanocrystals in aqueous solution via one-pot, biomimetic crystallization in nanopore assemblies. The key step of this process is to trigger the self-assembly of the nanopore with the metal ion, which generates supramolecular aggregates that mimic the biological crystal growth environment. The role of the nanopore building block is to promote nucleation of the constituent nanocrystals inside a porous matrix via coordination of metal ions to the carbonyl groups at the portals, and to control mass transport of the precursors of the reaction through the pores of the assemblies. The low specificity of the interaction between metal ions and the carbonyl groups of the nanopore paves the way for the utilization of the nanopore assemblies in the fabrication of nanocrystal superstructures of other functional materials such as CdS, ZnS, and PbS. This feature, along with the outstanding degree of accuracy observed in the alignment of the constituent nanocrystals, make this approach promising for the facile fabrication of self-organized structures with subnanometric resolution.

■ ASSOCIATED CONTENT

Supporting Information. Experimental Section, and Supporting Information Figures S1−S7. This material is available free of charge via the Internet at http://pubs.acs.org.

■ AUTHOR INFORMATION

Corresponding Author
roberto.delarica@gmail.com; a.h.velders@utwente.nl

■ ACKNOWLEDGMENT

The SRO Bionano of MESA+ is acknowledged for financial support. Mr. Enrico Keim and Mr. Mark Smithers are acknowledged for HRTEM imaging. We are thankful to Prof. Dr. A. Meijerink and Dr. D. Wasserberg for useful discussions.

■ REFERENCES

(1) Ridley, B. A.; Nivi, B.; Jacobson, J. M. *Science* **1999**, *286*, 746–749.
(2) Shevchenko, E. V.; Talapin, D. V.; Kotov, N. A.; O'Brien, S.; Murray, C. B. *Nature* **2006**, *439*, 55–59.
(3) Tao, A. R.; DeMartini, D. G.; Izumi, M.; Sweeney, A. M.; Alison, M.; Holt, A. L.; Morse, D. E. *Biomaterials* **2010**, *31*, 793–801.
(4) Hung, A. M.; Micheel, C. M.; Bozano, L. D.; Osterbur, L. W.; Wallraff, G. M.; Cha, J. N. *Nat. Nanotechnol.* **2010**, *5*, 121–126.
(5) Oaki, Y.; Kotachi, A.; Miura, T.; Imai, H. *Adv. Funct. Mater.* **2006**, *16*, 1633–1639.
(6) Song, R. Q.; Colfen, H. *Adv. Mater.* **2010**, *22*, 1301–1330.
(7) Addadi, L.; Joester, D.; Nudelman, F.; Weiner, S. *Chem.—Eur. J.* **2006**, *12*, 980–987.
(8) Niederberger, M.; Colfen, H. *Phys. Chem. Chem. Phys.* **2006**, *8*, 3271–3287.
(9) Kim, J.; Jung, I. S.; Kim, S. Y.; Lee, E.; Kang, J. K.; Sakamoto, S.; Yamaguchi, K.; Kim, K. *J. Am. Chem. Soc.* **2000**, *122*, 540–541.
(10) Lagona, J.; Mukhopadhyay, P.; Chakrabarti, S.; Isaacs, L. *Angew. Chem., Int. Ed.* **2005**, *44*, 4844–4870.
(11) Pejoux, C.; de la Rica, R.; Matsui, H. *Small* **2010**, *6*, 999–1002.
(12) Kitova, S.; Eneva, J.; Panov, A.; Haefke, H. *J. Imaging Sci. Technol.* **1994**, *38*, 484–488.
(13) Wang, H. J.; Yang, L.; Yang, H. Y.; Wang, K.; Yao, W. G.; Jiang, K.; Huang, X. L.; Zheng, Z. *J. Inorg. Biochem.* **2010**, *104*, 87–91.
(14) Hwang, I.; Jeon, W. S.; Kim, H. J.; Kim, D.; Kim, H.; Selvapalam, N.; Fujita, N.; Shinkai, S.; Kim, K. *Angew. Chem., Int. Ed.* **2007**, *46*, 210–213.
(15) Lee, T. C.; Scherman, O. A. *Chem. Commun.* **2010**, *46*, 2438–2440.
(16) Lu, X.; Masson, E. *Org. Lett.* **2010**, *12*, 2310–2313.
(17) Dabbousi, B. O.; Rodriguez-Viejo, J.; Mikulec, F. V.; Heine, J. R.; Mattoussi, H.; Ober, R.; Jensen, K. F.; Bawendi, M. G. *J. Phys. Chem. B* **1997**, *101*, 9463–9475.
(18) Du, Y.; Xu, B.; Fu, T.; Cai, M.; Li, F.; Zhang, Y.; Wang, Q. *J. Am. Chem. Soc.* **2010**, *132*, 1470–1471.
(19) Simon, P.; Carrillo-Cabrera, W.; Formanek, P.; Gobel, C.; Geiger, D.; Ramlau, R.; Tlatlik, H.; Budera, J.; Kniep, R. *J. Mater. Chem.* **2004**, *14*, 2218–2224.
(20) Wang, T.; Colfen, H.; Antonietti, M. *J. Am. Chem. Soc.* **2005**, *127*, 3246–3247.
(21) Aizenberg, J.; Black, A. J.; Whitesides, G. M. *Nature* **1999**, *398*, 495–498.
(22) Lee, S. Y.; Gao, X.; Matsui, H. *J. Am. Chem. Soc.* **2007**, *129*, 2954–2958.
(23) Samson, J.; Varotto, A.; Nahirney, P. C.; Toschi, A.; Piscopo, I.; Drain, C. M. *ACS Nano* **2009**, *3*, 339–344.